



**HAL**  
open science

# A NEW OPTIMIZATION ALGORITHM FOR A LI-ION BATTERY EQUIVALENT ELECTRIC CIRCUIT IDENTIFICATION

Rouba Al Nazer, Viviane Cattin, Pierre Granjon, Maxime Montaru

► **To cite this version:**

Rouba Al Nazer, Viviane Cattin, Pierre Granjon, Maxime Montaru. A NEW OPTIMIZATION ALGORITHM FOR A LI-ION BATTERY EQUIVALENT ELECTRIC CIRCUIT IDENTIFICATION. 9th International Conference on Modeling, Optimization & SIMulation, Jun 2012, Bordeaux, France. hal-00728565

**HAL Id: hal-00728565**

**<https://hal.science/hal-00728565>**

Submitted on 30 Aug 2012

**HAL** is a multi-disciplinary open access archive for the deposit and dissemination of scientific research documents, whether they are published or not. The documents may come from teaching and research institutions in France or abroad, or from public or private research centers.

L'archive ouverte pluridisciplinaire **HAL**, est destinée au dépôt et à la diffusion de documents scientifiques de niveau recherche, publiés ou non, émanant des établissements d'enseignement et de recherche français ou étrangers, des laboratoires publics ou privés.

## A NEW OPTIMIZATION ALGORITHM FOR A LI-ION BATTERY EQUIVALENT ELECTRICAL CIRCUIT IDENTIFICATION

R. AL NAZER, V. CATTIN

Commissariat à l'Energie  
Atomique Grenoble  
17 Rue des Martyrs  
38054 Grenoble Cedex – France  
[rouba.al-nazer@cea.fr](mailto:rouba.al-nazer@cea.fr),  
[viviane.cattin@cea.fr](mailto:viviane.cattin@cea.fr)

P. GRANJON

Gipsa-lab  
Grenoble Campus  
38402 SAINT MARTIN D'HERES  
France  
[pierre.granjon@gipsa-lab.grenoble-inp.fr](mailto:pierre.granjon@gipsa-lab.grenoble-inp.fr)

M. MONTARU

INES CEA Laboratoire Stockage  
de l'Electricite  
CEA - INES RDI, Lynx 1, 50 av  
du lac Lemman, BP332, 73377 Le  
Bourget du Lac Cedex, France  
[maxime.montaru@cea.fr](mailto:maxime.montaru@cea.fr)

**ABSTRACT:** *An equivalent electrical circuit (EEC) is commonly used to model the electrochemical aspect of a battery. Its structure can be more or less complicated depending on the needs of the application. Impedance measurements obtained by electrochemical impedance spectroscopy need non integer order impedance in order to correctly model passivation film and diffusion phenomena. Identification of the parameters of the EEC from electrochemical spectroscopy is difficult because of non unicity of the solution and lack of convergence of standard algorithms. The study of the experimental measurements shows that each chemical phenomenon is sollicitated in a precise waveband. We propose thus three approaches to improve the identification convergence depending on whether / how we introduce information on the frequency or not. In the first one, we identify all the parameters in the whole waveband (classical approach). The second and third ones (alternative approaches) split the waveband and identify only the corresponding excited parameters. In all these cases, the identification of the parameters of the EEC should use a non linear method and must lead to an accurate result. The Levenberg-Marquardt algorithm is adopted in this study. A statistical study shows that the first approach can't converge strongly while the second and third one converge with the presence of a bias. Thus we propose to adopt a new method of identification based on a two-steps algorithm.*

**KEYWORDS:** *optimization method, Levenberg-Marquardt algorithm, battery modelling, equivalent electrical circuit, electrical impedance spectroscopy, battery monitoring system.*

### 1 INTRODUCTION

The battery is a critical element in HEV (*hybrid electric vehicle*) as in EV (*electric vehicle*). The lithium ion battery has several advantages among other technologies, such as high power density and high energy density (Wakihara M. and Yamamoto O., 2008) (Kazunori O., 2009). Thus, it is an excellent candidate for the HEV and EV applications. Due to its frequent charges and discharges, a BMS (*Battery Management System*) becomes very important. The BMS is necessary to predict the battery SOC (*State Of Charge*), SOH (*State Of Health*) and finally ensure security. These factors are generally used to diagnose and manage the battery states, and to increase its lifetime and reliability. Until now, various methods and models have been proposed to predict these states. For example, diverse equivalent electrical circuits have been used to modelize Li-ion battery behaviour. However, accurate description of the complex nonlinear electrochemical processes occurring in such systems is still difficult.

This paper focuses on the identification of an equivalent electrical circuit whose parameters are scheduled on the SOC, temperature, and current intensity and direction. This equivalent electrical circuit (EEC) introduces non

integer derivatives to accurately modelize the Li-ion battery behaviour. We propose to identify the EEC parameters with a new double steps algorithm, which improves the rate of convergence usually obtained for this optimization problem. The validity of the procedure is demonstrated experimentally for an A123 lithium ion iron-phosphate battery inside a large range of values of current intensity and state-of-charge.

### 2 BATTERY MODELS

Modelling aims to reproduce the electrical behaviour of batteries through equivalent electrical circuits consisting of passive (resistors, capacitors, inductors, constant phase elements) and active (voltage and current sources) elements. For electrical engineers, such circuits are common to characterize electrochemical phenomena, and they lead to perform a quick analysis and prediction of the battery behaviour in frequency as in time domains. A large variety, more or less complex, of equivalent electrical circuits is found in the literature. In the next section we present some of the most known models (Urbain M., 2009).

## 2.1 The basic Thevenin type model

The simplest model (Figure 2-1) consists of a voltage source (OCV for *Open Circuit Voltage*) and a resistance  $R$  in series. The variability of these parameters with the effect of the state of charge and temperature could be taken into account by tabulation or empirical law. However, this model does not modelize the dynamical behavior of battery voltage. Nevertheless, it can be very useful for some applications, especially for application with low variations of current sollicitation .

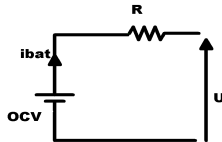


Figure 2-1: The basic Thevenin type model

## 2.2 The first order Thevenin type model

This model enhances the previous one. It introduces a  $R1/C1$  element in series with  $R$  to modelize dynamical phenomena that occur in a battery while charging or discharging (Figure 2-2).

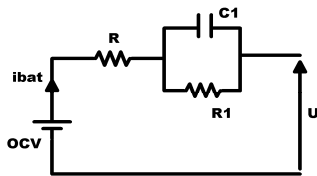


Figure 2-2: First order Thevenin type model

## 2.3 PNVG (Partnership for a New Generation of Vehicles) Thevenin type model

This model (Urbain M., 2009) introduces a new capacity  $1/OCV'$  to take into account the variation of the open circuit voltage with respect to the state of charge (Figure 2-3). We can note that a tabulation of OCV with SOC could have offered the same functionality without adding this component.

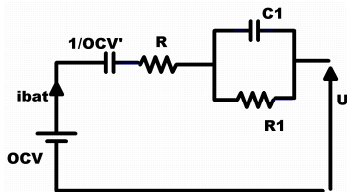


Figure 2-3: PNVG Thevenin type model

## 2.4 Adapted Randles model

This is the model adopted in our study (Figure 2-4). It was developed and used in the work led by DONG K.

(Dong K., 2010). It includes the modelization of connectors and electrolyte, passivation film, charge transfer and double layer phenomena. The OCV is given in a look up table with respect to the current intensity and the battery state of charge . This circuit introduces constant phase elements (CPE) to accurately reflect the behaviour of the battery observed on impedance spectroscopy measurements. (Oustaloup A., 1995) (Oustaloup A., 2005). A CPE is a component that traduces a partially capacitive and resistive behaviour. It includes two parameters  $T$  and  $p$ , where  $0 \leq p \leq 1$ , its impedance is given by Eq. (1). As it can be noted, the corresponding component is a capacitor for  $p = 1$  and a pure resistance for  $p = 0$ .

$$Z_{CPE}(f) = \frac{1}{T(j2\pi f)^p} \quad (1)$$

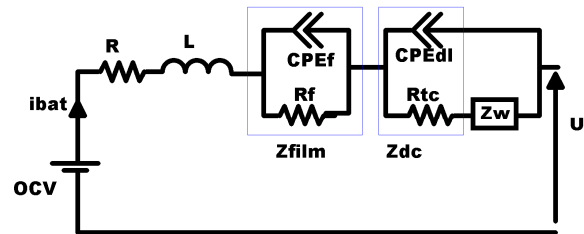


Figure 2-4: Adapted Randles model

### 2.4.1 Electrolyte and connectors impedances

The passage of any current through the battery comes along with voltage drops due to connectors and electrolyte resistance. Although these resistances are weak, they are the main cause of Joule losses inside the battery. Consequently, they are modelized in this EEC thanks to the parameter  $R$ . Identifying resistive (dissipative) elements in the equivalent circuit makes the link between a purely dynamic model and a thermal one. Due to the connectors, an inductive behaviour is observed while exciting the battery with high frequencies. This leads to introduce an inductance  $L$  in series with the resistance  $R$  to modelize this phenomenon (Kuhn E., Forgez C. and Friedrich G., 2004).

### 2.4.2 Double layer capacitance

The double layer capacitance is the electrical representation of the electrode-electrolyte interface, which is proportional to the area of the electrode plate. In this electrical circuit, the double layer capacitance is modelized through the constant phase element  $CPE_{dl}$  (Kuhn E., Forgez C. and Friedrich G., 2004).

### 2.4.3 Charge transfer phenomena

Charge transfer phenomena correspond to the flux of oxydising and reducing species from one electrode to another (Kuhn E., Forgez C. and Friedrich G., 2004). As in the first order Thevenin type model, they are modelled

by a resistance  $R_{tc}$  in parallel with the previous double layer component.

#### 2.4.4 Diffusive phenomena

During charge and discharge cycles, concentration gradients of electroactive species appear which bring about mass transport phenomena and thus modify electrochemical potentials. Such phenomena are peculiarly active when the cell is operated in very low frequencies, or in high currents (Kuhn E., Forgez C. and Friedrich G., 2004). Diffusion is more important as electrodes potentials differ strongly from their equilibrium values, and mostly appears at very low frequencies. Generally, this phenomenon is modelled by a transfer function called "Warburg Impedance", noted  $Z_w$  in Figure 2-4. In this study we consider higher frequencies and neglect such phenomenon (Dong K., 2010).

#### 2.4.5 Passivation film

When the potential of negative electrodes (resp. positive) is located outside the field of electrochemical stability, a partial reduction (resp. decomposition) of the electrolyte on the surface of the active material is then observed. This process involves the use of a portion of lithium and creates a solid layer on the surface of these electrodes, called "passivation film". In addition to an irreversible decrease in the capacity of the battery, the presence of this layer induces a decrease in available power due to the increase of the impedance of the electrode (Dong K., 2010). A branch  $R_f/CPE_f$  is used to modelize these complex phenomena.

Finally, the adopted electrical equivalent circuit (Figure 2-4) consists of eight parameters [ $R$ ;  $L$ ;  $R_f$ ;  $T_f$ ;  $P_f$ ;  $R_{tc}$ ;  $T_d$ ;  $P_d$ ] that should be optimized in order to correctly modelize the battery's behaviour. This is the aim of the next sections.

### 3 ELECTRICAL EQUIVALENT CIRCUIT IDENTIFICATION

Electrochemical Impedance Spectroscopy (EIS) is a commonly used method to characterize electrochemical systems (Buller S., 2002). After a brief reminder of EIS applications in battery modelling, we will describe how the parameters of the EEC can be estimated thanks to this technique.

#### 3.1 An overview of impedance spectroscopy

Impedance Spectroscopy is an experimental technique generally used as impedance characterization. The principle of EIS is the following (Gabrielli C., 1996): when adding a small sinusoidal current of frequency  $f$   $i(t) = I_{\max} \sin(2\pi ft)$  to a DC current at the input of the battery under test, its voltage response is

$v(t) = V_{\max} \sin(2\pi ft - \varphi)$ . Therefore, we can express the voltage/current ratio in the frequency domain as a complex impedance as in equation (2):

$$Z_{est}(f) = \frac{V_{\max}}{I_{\max}} * \exp(-j\varphi) \quad (2)$$

Since batteries are in general non linear systems, a constraint is set on  $I_{\max}$  to avoid charge modification during measurement. This mode of operation is known as the galvanostatic mode, by opposition to the potentiostatic mode where the battery voltage is the input and its current the output. When applying this method to a set of different frequencies, we obtain the so-called "Impedance Spectrum", a complex number  $Z_{est}(f)$  depending on the frequency  $f$  and whose theoretical shape is shown in Figure 3-1 (a).

It is clear from Figure 3-1 that the EEC presented in Figure 2-4 is able to accurately modelize a true battery impedance spectrum (Figure 3-1 (b)) if its parameters are correctly optimized. The optimization procedure is described in the next section.

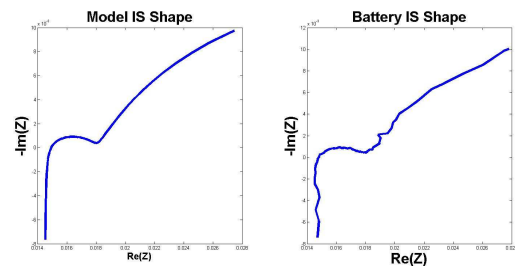


Figure 3-1: (a) A simulated EEC impedance spectrum  
(b) An experimental Li-Ion battery impedance spectrum

#### 3.2 EEC parameters identification and optimization

From experiential data, we define the identification by the search for mathematical models of the battery system. These models provide an approximation as accurate as possible of the behaviour of the underlying physical system in order to estimate the physical parameters and to design algorithms for simulation, supervision, diagnosis and control. The identification usually starts with a plan of experiments where the inputs/outputs are determined and measured and where the excitation signals are selected. Following this first step, a model is selected among linear candidates or not, taking into account the noise or not. From the chosen error signal, a condition is then selected from the different types of existing criteria (quadratic, absolute value, maximum likelihood, AIC, Young, Bayesian...). The estimation of the parameters is then achieved by minimizing this criterion. Techniques based on linear programming, such as least squares and instrumental variable, or based on nonlinear programming, such as the gradient method and all its variants, are commonly used. Finally, the resulting model is validated or invalidated by the tests.

In our study, the model is composed of the impedance of the equivalent electrical circuit. The input is the battery current which is a sinusoid of variable frequency added to a DC component, and the output is the measured battery voltage. The criterion to minimize is the mean squared value of the error given by equation (3). This error corresponds to the difference between the phase and the logarithmic modulus of the impedance predicted by the model  $Z_{est}$  and those obtained through measurements  $Z_n$ .

$$E(f) = \left( \begin{array}{l} \ln(|Z_n(f)|) - \ln(|Z_{est}(f)|) \\ phase(Z_n(f)) - phase(Z_{est}(f)) \end{array} \right) \quad (3)$$

Where:  $Z_n$ :  $Z_{simulated+noise}$  Or  $Z_{measured}$   
 $Z_{est}$ :  $Z$  estimated by the model

This method leads to a non-linear least squares optimization problem, whose optimal solution can be obtained thanks to the Levenberg-Marquardt algorithm (Canat S., 2009).

This approach is summarized in Figure 3-2.

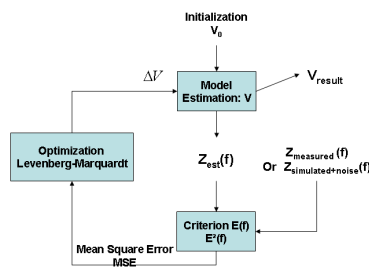


Figure 3-2: Optimization method

The convergence properties of this algorithm are reflected by the output parameter "exitflag" whose values are explained in Table 3-1 : Exitflag values..

Value	Signification
1	Function exactly converged to a stable solution x.
2	Change in x between two iterations was less than the specified tolerance TolX ( $10^{-15}$ ).
3	Change in the criterion between two iterations was less than the specified tolerance TolFun ( $10^{-100}$ ).
0	Number of iterations exceeded MaxIter (400)

Table 3-1 : Exitflag values.

The theoretical study of the convergence properties is out of the scope of this paper because the criterion that has to be minimized is strongly nonlinear, and presents many local minima. Therefore, these properties heavily depend on the initial vector value.

In what follows, different ways to use the Levenberg-Marquardt algorithm and to efficiently solve this optimization problem will be detailed in the next sections, and a statistical study is used to analyze the convergence properties of the proposed algorithms.

### 3.2.1 Classical approach

The classical approach consists of identifying all the EEC parameters in the whole frequency band.

To test the performance of this method, a statistical study is performed. Starting with a known vector of parameters, a complex impedance  $Z(f)$  is generated using a large amount of frequencies (from 5 mHz to 65 kHz). A complex-valued white noise is added to this theoretical impedance in order to modelize measurement noise. One hundred iterations of such noisy impedances are generated with the same signal to noise ratio. For each iteration, an initial vector is arbitrary chosen within limited values (Table 3-2). The results show that with such a method, the convergence of the Levenberg-Marquardt algorithm is not guaranteed: this method is very affected by the choice of the initialization vector. An expert knowledge of specialists in batteries is required to correctly initialize the initial vector in order to improve the convergence rate of this algorithm and to accurately estimate the theoretical vector.

Two criteria are used to compare the results: the relative mean errors RME (4) and the convergence rate CR (5).

$$RME = 100 * \frac{(\text{mean}(V_{est}) - V_{sim})}{V_{sim}} \quad (4)$$

where  $V$  is one of the elements  $[R; L; R_f; T_f; P_f; R_c; T_{dl}; P_{dl}]$

$$CR = \frac{\text{Convergent iterations}}{\text{total number of iterations}} \quad (5)$$

In Table 3-3 we present the RME (min and max) and the convergence rate for two cases : for the first one, the initial vector is selected without any expert knowledge of the batteries while for the second one, it was chosen carefully. In that case, the true parameters value should be approximately known.

	Theoretical Value	Initial vector (expert knowledge case)	Upper_bound (low a priori knowledge case)
R (Ohm)	0.0130	$10^{-2}$	1
L (H)	$4 \times 10^{-8}$	$10^{-8}$	$10^{-6}$
Rf (Ohm)	0.004	$10^{-3}$	1
Tf	5.7	5	10
Pf	0.53	0.1	1
Rtc (Ohm)	0.04	$10^{-2}$	1
Tdl	700	100	1000
Pdl	0.7	0.1	1

Table 3-2 : Numeric values used on the simulation. The last column is used to generate a arbitrarily initial vector within  $[0 \text{ Upper\_bound}]$  limits.

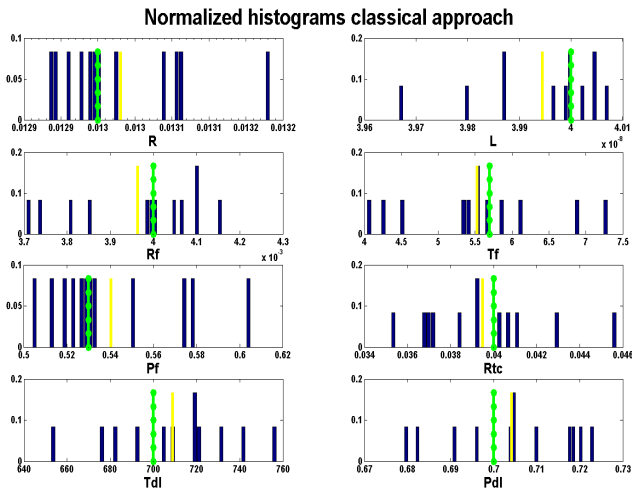


Figure 3-3: Normalized histograms using the classical approach with an arbitrarily initial vector (green lines = theoretical values, yellow lines = estimated mean values)

These results clearly show that less we know about the EEC parameters value, less the algorithm converges to the exact values. In

Figure 3-3 we present the normalized histograms corresponding to the first case for the eight components of the chosen EEC (Figure 2-4)- The green lines refer to theoretical parameters values while the yellow ones refer to mean parameters values estimated over all the iterations where the algorithm converged.

### 3.2.2 Alternative approaches

As we said before, in an identification process, an *a priori* knowledge of the system can be injected. Figure 3-4 shows that the part of the EEC which is excited by the input current depends on the input frequency. For example, passivation film effects only appear for frequencies lower than 10 kHz (see the green curve) while the double layer and charge transfer are only important for frequencies lower than 1 Hz (see the red curve). We can also note that the electrolyte and connectors impedance modeled by R and L are only dominating in the high-frequency band (see the blue curve, for frequencies higher than 10 kHz).

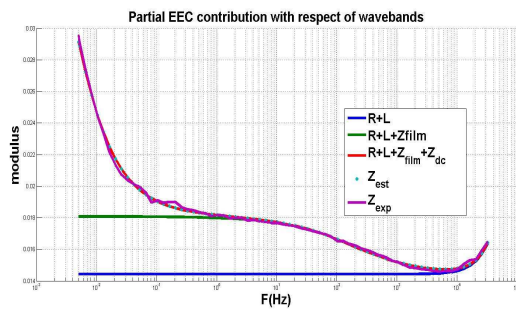


Figure 3-4: Partial theoretical impedance modulus compared with an experimental impedance modulus

This observation leads us to propose two alternative approaches to use this *a priori* knowledge in the optimization process.

#### a) Frequency band segmentation

In this approach, we split the whole frequency band in different parts and identify the excited parameters in the frequency band where their impedance is important (ie the parameters excited in low frequency band are identified using only low frequencies, those excited in medium frequency band using medium frequencies, and those excited in high frequency band using only high frequencies).

#### b) Frequency band extension

In this second approach, we also split the whole frequency band in three parts, but during each step we extend the limits of the intervals of frequencies (ie the parameters excited of the medium waveband are identified using the low and medium frequencies, and those excited in high waveband using all the frequencies).

The main difference between the classical approach and these two alternative approaches is located in the nature of the *a priori* knowledge necessary to make the optimization algorithm converge. For the classical approach, the initial vector of EEC parameters has to be set with values close to the true ones. Unfortunately, this kind of knowledge is only accessible to expert people. For the proposed alternative approaches, only the approximate values of the different frequency bands has to be known, which is a much more simple knowledge to obtain. A statistical test similar to the one done in section 3.2.1 has been done to study the performance of these alternative approaches. The obtained results (Figure 3-5 and Figure 3-6) prove that these alternative approaches strongly enhance the rate of convergence, but the estimated parameters are then biased. As it is shown in Table 3-4, the frequency band segmentation approach leads to better results than the extension one in term of bias, with an equivalent convergence rate.

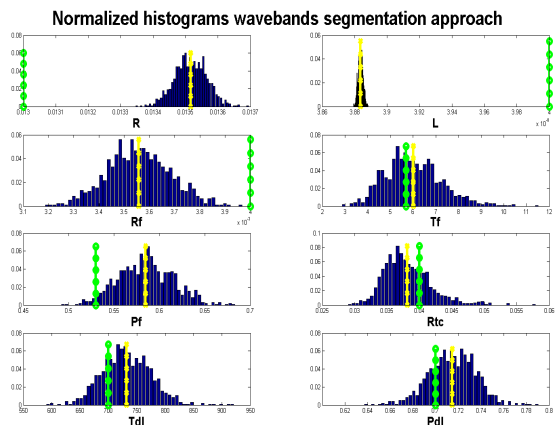


Figure 3-5: Normalized histograms using frequency band segmentation approach (green lines = theoretical values, yellow lines = estimated mean values)

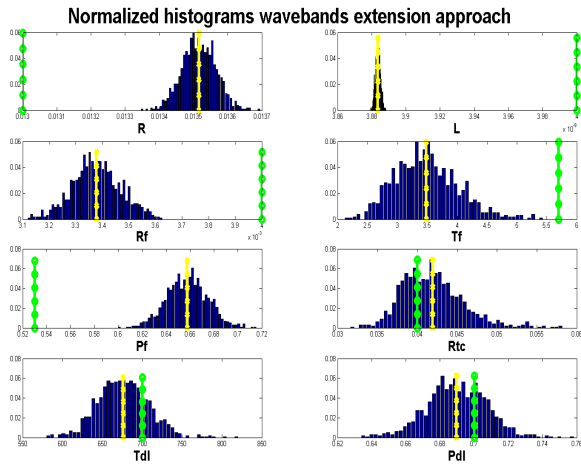


Figure 3-6 Normalized histograms using frequency band extension approach (green lines = theoretical values, yellow lines = estimated mean values)

### 3.2.3 The new approach: two-steps identification

Based on the previous results, a new algorithm has been elaborated; it is called « identification in two steps with an *a priori* knowledge in the frequency domain ». The principle is based on the fusion of the classical approach and the frequency band segmentation one in order to make use of their respective advantages. As a first step, we use the frequency band segmentation approach. The resulted identified vector of parameters will be used as the initial vector of the second step while applying the classical approach. And thus we make use of the high convergence rate of the segmentation approach and of the estimation accuracy of the classical one. Once again, a statistical study is done to evaluate the performance of this new approach. The results shown in Figure 3-7 and Table 3-5 prove that the identification process is achieved with a high convergence rate and an enhanced relative mean error rate. The bias of the identified parameters is less than 1 % for 96 % of all the cases.

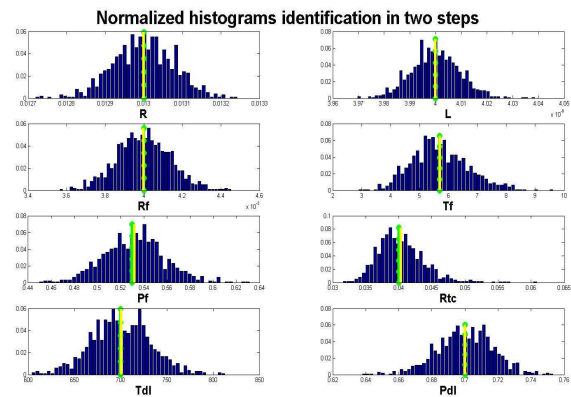


Figure 3-7: Normalized histograms using the two-steps identification method (green lines = theoretical values, yellow lines = estimated mean values)

Initial vector	RME in % [min,max]	Convergence rate
Low a priori knowledge	[ 0.2 , 3 ]	2 %
Expert knowledge	[0.006 , 0.4]	30%

Table 3-3: Relative mean errors and convergence rates (1<sup>st</sup> row: arbitrary initial vector; 2<sup>st</sup> row: initial vector selected with expert knowledge)

Alternative approach	RME in % [min,max]	Convergence rate
frequency band segmentation	[ 2 , 11 ]	96 %
frequency band extension	[ 2 , 30 ]	96%

Table 3-4: Relative mean errors and convergence rates (alternative approaches)

	RME in % [min,max]	Convergence rate
new approach	[ $2 \times 10^{-4}$ , 0.7 ]	96 %

Table 3-5: Relative mean errors and convergence rate using the two-steps identification method

### 3.3 Experimental Results

In order to validate the new algorithm, we used it to identify a set of experimental spectrometry data. The results prove that this algorithm is able to correctly identify the true battery spectrum impedance. It had been tested on a large amount of available experimental data for different current intensities and different states of charge. Figure 3-8 shows the results for few cases. It is important to note that the variability of the EEC parameters with respect to charge/discharge current and to SOC has been the subject of the study realized by Dong (Dong K., 2010)( Dong K., 2011).

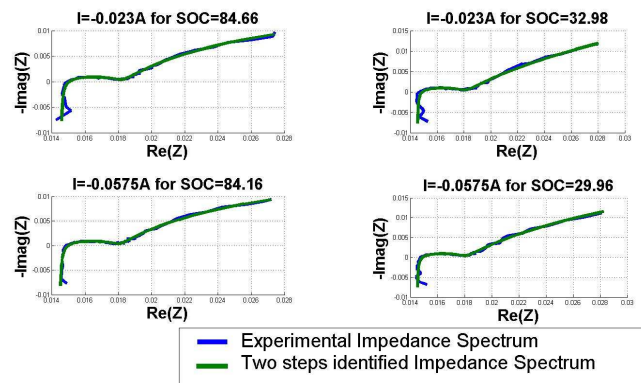


Figure 3-8: Experimental and estimated impedance spectrum for two different current intensities and SOC's

#### 4 CONCLUSION AND FUTURE WORKS

In this work, a new optimization method has been proposed in order to accurately estimate the parameters of a battery EEC from experimental impedance measurements. This method consists of a two-steps optimization algorithm. It reaches high convergence rates and good estimation performance without the need of expert *a priori* knowledge concerning EEC parameters values. In future works, this method needs to be extended to characterize a pack of batteries, and a real time version will be developed to be used for automotive on-board applications.

#### REFERENCES

- Buller S., 2002. *Impedance-Based Simulation Models for Energy Storage Devices in Advanced Automotive Power Systems*, Thèse de Doctorat,.
- Canat S., 2009. *Contribution à la modélisation dynamique d'ordre non entier de la machine asynchrone à cage*. Thèse de Doctorat, Institut National Polytechnique de Toulouse, France.
- Dong K., 2010. *Contribution à la modélisation dynamique des batteries Lithium-ion pour l'application photovoltaïque et stockage connecté au réseau*. Thèse de Doctorat, Institut Polytechnique de Grenoble, France.
- Dong K., 2011. *Dynamic Modeling of Li-Ion Batteries Using an Equivalent Electrical Circuit*. Journal of the Electrochemical Society, 158 (3) A326-A336.
- Gabrielli C., 1996. *Techniques de l'ingénieur* PE 2 210.
- Kazunori O., 2009. *Lithium Ion Rechargeable Batteries : Materials, technology and new applications*.
- Kuhn E., Forgez C. and Friedrich G., 2004. *Modeling diffusive phenomena using non integer derivatives*. The European Physical Journal Applied Physics, V25, p. 183-190.
- Oustaloup A., Hermes Sciences Publicat, 1995. *La dérivation non entière : Théorie, Synthèse et Applications*.
- Oustaloup A., Hermès-Lavoisier, 2005. *Représentation et identification par modèle non entier*.
- Urbain M., 2009. *Modélisation électrique et énergétique des accumulateurs Lithium-In. Estimation en ligne du SOC et SOH*. Thèse de Doctorat, Institut National Polytechnique de Lorraine, France.